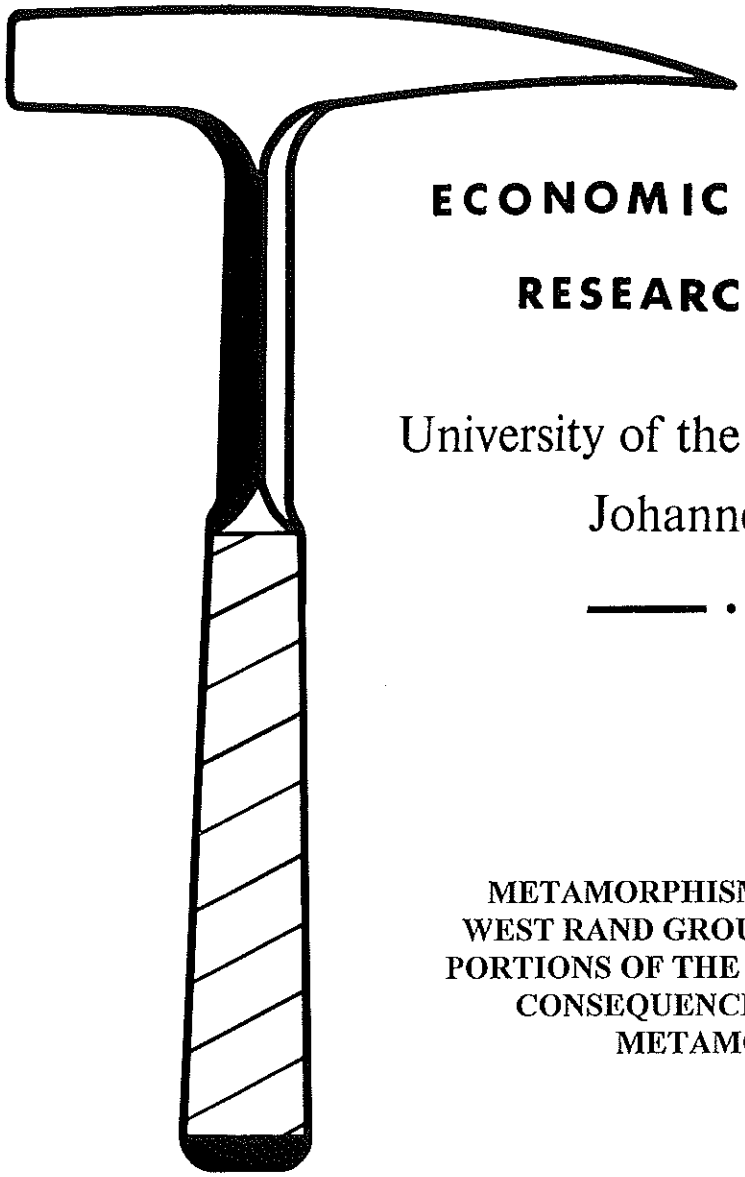

ECONOMIC GEOLOGY

RESEARCH UNIT

University of the Witwatersrand

Johannesburg

METAMORPHISM AND ALTERATION OF WEST RAND GROUP SHALES FROM DISTAL PORTIONS OF THE WITWATERSRAND BASIN: CONSEQUENCES FOR A BASIN-WIDE METAMORPHIC MODEL

ROBIN PRESTON and GARY STEVENS

INFORMATION CIRCULAR No. 325

UNIVERSITY OF THE WITWATERSRAND
JOHANNESBURG

METAMORPHISM AND ALTERATION OF WEST RAND GROUP SHALES FROM DISTAL PORTIONS OF THE WITWATERSRAND BASIN: CONSEQUENCES FOR A BASIN-WIDE METAMORPHIC MODEL

by

ROBIN PRESTON and GARY STEVENS
(Economic Geology Research Unit, University of the Witwatersrand, Private Bag 3, WITS 2050, South Africa)

ECONOMIC GEOLOGY RESEARCH UNIT
INFORMATION CIRCULAR No. 325

August, 1998

METAMORPHISM AND ALTERATION OF WEST RAND GROUP SHALES FROM DISTAL PORTIONS OF THE WITWATERSRAND BASIN: CONSEQUENCES FOR A BASIN-WIDE METAMORPHIC MODEL

ABSTRACT

This paper documents the metamorphism and alteration in West Rand Group shales exposed in three boreholes east and south of the Vredefort Dome. In all the samples studied, the maximum metamorphic grade is lower greenschist facies. In most cases, the peak metamorphic assemblage consists of quartz + muscovite + chlorite, with the phyllosilicates defining a tectonic cleavage. In many of the samples coarsely crystalline alteration zones crosscut both the bedding and the tectonic cleavage, clearly overprinting these structures. The alteration zones are localized around minor faults and shears where fluid ingress has occurred. Muscovite was not observed in these zones and the cleaved matrix assemblages has been replaced by assemblages consisting of pyrite + quartz ± chlorite ± stilpnomelane ± calcite ± carbonaceous matter ± Mn-garnet ± epidote ± chalcopyrite. In several alteration zones stilpnomelane is a common product and appears to arise through the breakdown of chlorite + muscovite. Attempts to balance this reaction using measured mineral compositions were unsuccessful assuming an isochemical system. Major mobility of K and Fe is implied, as well as the obvious mobility of S, Cu and C. Assays on small samples indicated gold introduction into the shales during the alteration event. Chlorite thermometry was used to estimate the equilibration temperature of chlorite from the cleaved matrix and the alteration zones. Temperatures close to 300 °C were indicated for chlorites from both of these settings and for all three boreholes. These results, and the petrographic data, imply that fluid influx post-dated the formation of the tectonic cleavage, but occurred close to the peak of metamorphism. Comparison between the chlorite thermometry data from this study with that from similar studies in the goldfields indicates analogous peak metamorphic grades in both areas, suggesting that these metamorphic conditions may be typical of almost the entire Witwatersrand Basin. An exception is the amphibolite facies metamorphism exposed in the West Rand Group strata of the northwestern sector of the collar of the Vredefort Dome. Several recent studies have suggested that this metamorphism is representative of a widespread zone of higher grade conditions within the central portions of the Basin which formed in response to a generally elevated crustal geotherm during Bushveld magmatic activity. The present study indicates that this suggested high grade metamorphic zone does not extend east and south of the Vredefort Dome and consequently, it is proposed that the amphibolite facies rocks exposed in the northwestern sector of the Vredefort collar are probably unique to this segment of the Dome.

_____oOo_____

METAMORPHISM AND ALTERATION OF WEST RAND GROUP SHALES FROM DISTAL PORTIONS OF THE WITWATERSRAND BASIN: CONSEQUENCES FOR A BASIN-WIDE METAMORPHIC MODEL

CONTENTS

_____oOo_____

Published by the Economic Geology Research Unit
Department of Geology
University of the Witwatersrand
1 Jan Smust Avenue
Johannesburg 2001
South Africa

ISBN 1-86838-216-8

METAMORPHISM AND ALTERATION OF WEST RAND GROUP SHALES FROM DISTAL PORTIONS OF THE WITWATERSRAND BASIN: CONSEQUENCES FOR A BASIN-WIDE METAMORPHIC MODEL

INTRODUCTION

Recently, the metamorphism and alteration of the rocks of the Witwatersrand Basin have been the subject of considerable research attention. Several studies have documented alteration processes that operated on a variety of scales in the goldfields located along the northern and north-western margins of the Basin (e.g., Phillips and Myers, 1989; Robb and Meyer, 1991; Robb and Meyer, 1995; Frimmel *et al.*, 1993; Fox and Winkler, 1997; Barnicoat *et al.*, 1997; Phillips *et al.*, 1997a). Similarly, advances have been made in the understanding of the metamorphic history of this portion of the Basin. The peak metamorphic conditions exposed along 300 km of the northern and north-western Basin margin have been established at between 300 and 350 °C (Phillips, 1987a; Wallmach and Meyer, 1990; Frimmel *et al.*, 1993; Zhou and Phillips, 1994; Zhou *et al.*, 1994; Phillips *et al.*, 1997b).

Despite these investigations, there remains considerable debate about the ultimate timing, causes and scale of both the metamorphic and alteration processes, as well as the relationship of the metamorphism in this area to that in the wider basin as a whole. In this regard, Gibson and Wallmach (1995), Stevens *et al.* (1997a) and Phillips *et al.* (1997a) have argued that the low-grade metamorphism in the Witwatersrand Basin was the consequence of a more widespread thermal event that affected much of the Kaapvaal Craton, and have linked this metamorphism to that in the Witwatersrand rocks and their associated basement exposed within the Vredefort Dome. These authors proposed that the peak metamorphic event throughout the Basin resulted from a period of high heat flux as a consequence of widespread magmatic activity at the time of the intrusion of the Rustenburg Layered Suite and the Lebowa Granite Suite, and the extrusion of the Rooiberg lavas. In this interpretation, a large portion of the central Witwatersrand Basin is seen to be metamorphosed to between upper greenschist and mid-amphibolite facies conditions. Stevens *et al.* (1997a) proposed that metamorphic fluids liberated from West Rand Group shales during this event contributed significantly to alteration and gold mobilisation in the Central Rand Group rocks exposed in the Witwatersrand goldfields. This metamorphic model remains to be tested using data from areas outside of the Vredefort Structure, as well as by rigorous geochronological studies on metamorphic rocks within the structure. This undertaking is largely hampered by the availability of exposure, as almost all of the central and south-eastern portions of the Basin are covered by post-Witwatersrand strata. In addition there are added difficulties associated with dating specific events in rocks with complex metamorphic histories (cf. Gibson and Wallmach, 1995; Reimold *et al.*, 1996; Stevens *et al.*, 1997b).

This study sets out to contribute to the understanding of metamorphism in the Witwatersrand Basin by detailing the metamorphic and alteration histories of West Rand Group shales exposed in boreholes from the southeastern portions of the Basin, and from within the collar of the buried, southern portion of the Vredefort Structure.

GEOLOGICAL SETTING

The Witwatersrand Supergroup represents part of a succession of late Archaean to Proterozoic supracrustal rocks deposited on the granitoid-greenstone basement of the

Kaapvaal Craton . Deposition commenced around 3,07 Ga, through subaerial extrusion of the mafic volcanic rocks of the Dominion Group. This was followed by the deposition of the siliciclastic sediments of the Witwatersrand Supergroup, consisting of a lower argillaceous to arenaceous subtidal marine sequence, the West Rand Group, and an upper fluvial and alluvial - fan dominated sequence, the Central Rand Group. Mafic volcanic rocks of the 2,7 Ga Ventersdorp Supergroup overlie the Witwatersrand succession. Ventersdorp magmatism was followed by the deposition of the 2,6 – 2,2 Ga Transvaal Supergroup, comprising a lower dolomitic sequence; the Chuniespoort Group, and the upper transgressive, marine - dominated Pretoria Group. Widespread intracratonic mafic and felsic magmatism followed the termination of Transvaal sedimentation. This magmatic episode was manifested in the eruption of the volcanic rocks of the Rooiberg Group, contemporaneous with the emplacement of the mafic - to - ultramafic Rustenburg Layered Suite into the upper levels of the Transvaal Supergroup at approximately 2.06 Ga. The final pulses of magmatism resulted in the late-stage emplacement of the Lebowa Granite Suite into the Rustenburg Layered Suite.

At approximately 2.02 Ga, the Witwatersrand Basin and overlying sequences suffered widespread deformation associated with the formation of the Vredefort Dome. Field observations, together with micro-scale deformation features and mineral associations involving high - pressure quartz polymorphs (cf. review of Reimold and Gibson, 1996) has led to widespread acceptance that the Dome formed during a catastrophic meteorite impact event. The Vredefort Dome exposes a core of pre-Dominion, Archaean granitoid basement and a collar of steeply dipping to overturned strata represented by Dominion Group and Witwatersrand, Ventersdorp and Transvaal Supergroup rocks.

Metamorphism and Alteration in the Witwatersrand Basin

Only during the last decade has research on Witwatersrand rocks begun to include studies specifically targeted at understanding the role of metamorphism and alteration in the evolution of the Basin. This has been brought about by the realization that the rocks of the Basin are metamorphic rocks; that the peak metamorphic minerals, particularly in reef horizons in the goldfields, are indicative of an altered bulk rock geochemistry; and, that a significant proportion of the gold in the Basin is associated with conglomeratic reef packages and has been precipitated from a fluid phase.

Reports of metamorphic mineral assemblages in the largely conglomeratic "reef packages" of the goldfields date from as early as Young (1917). However, it was only following the work of Phillips (1987a) that a systematic approach was adopted to address the question of metamorphism in the goldfields around the northern margin of the Basin. Phillips showed that all the goldfields experienced a similar, regional, lower greenschist facies metamorphism that in the metasediments, resulted in the development of minerals such as pyrophyllite, chloritoid, muscovite, chlorite and quartz (Fig. 1). Subsequent studies have confirmed Phillips' estimates of pressure-temperature conditions of ~350 ± 50 °C, 2-3 kbar for the metamorphic peak (e.g., Wallmach and Meyer, 1990; Frimmel, 1994; Zhou *et al.*, 1994). In a few areas around the goldfields, slightly higher-grade assemblages involving kyanite, andalusite, cordierite and/or biotite have been reported in the Witwatersrand Supergroup (e.g., Schreyer and Bisschoff, 1982; Tweedie, 1986; Phillips, 1987a; Phillips and Law, 1994). In general, these higher metamorphic grades have been interpreted to be the result of heating effects emanating from the Bushveld Complex (Schreyer and Bisschoff, 1982), or from intrusions of Bushveld age (Tweedie, 1986).

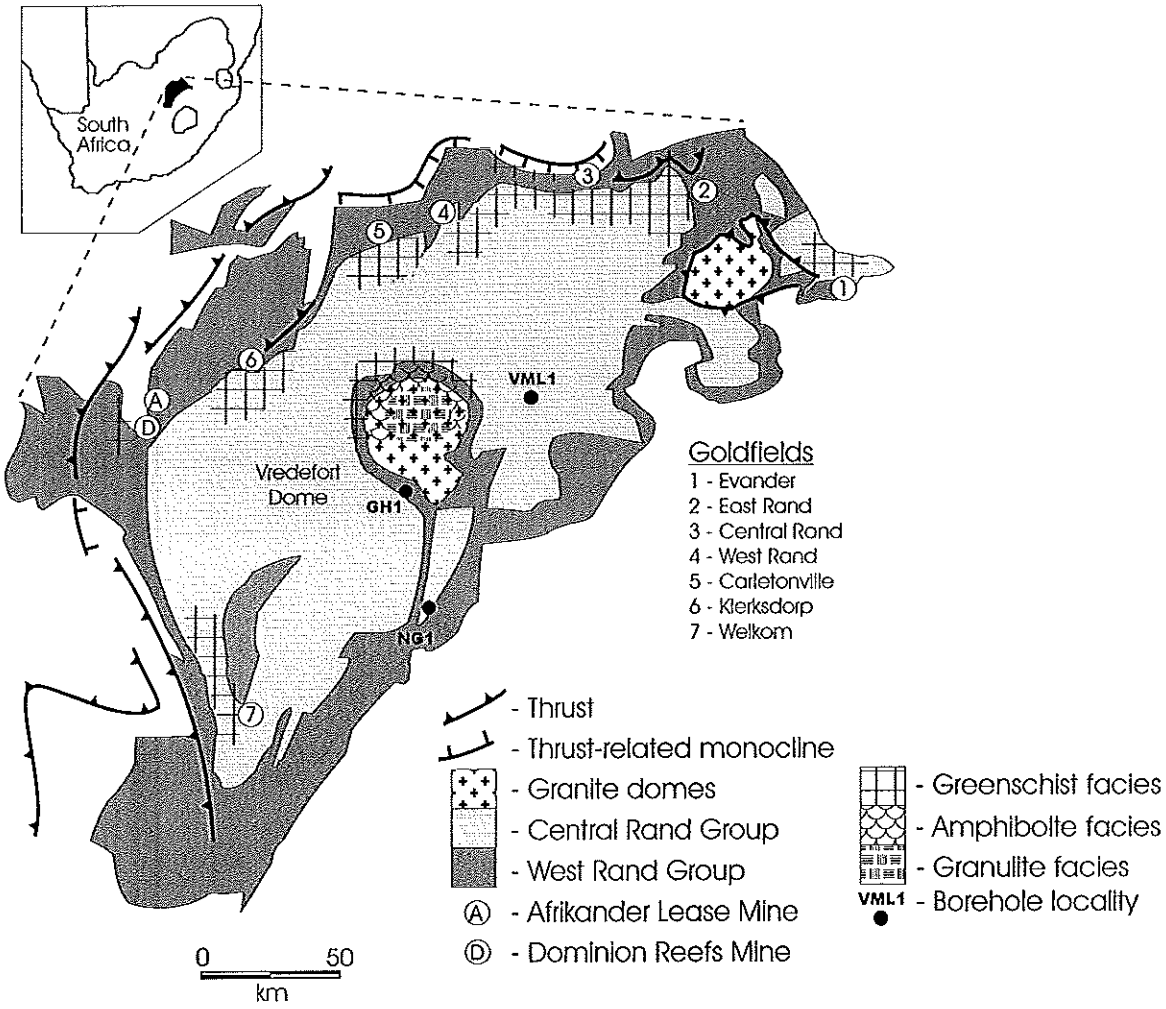

Figure 1: Simplified geological map of the Witwatersrand Basin and the Vredefort Dome illustrating the known distribution of metamorphic facies in areas of exposure or mining activity.

Chloritoid + pyrophyllite + quartz occurs as the peak metamorphic assemblage within many reef packages and within argillaceous partings in reefs (Phillips, 1988). Kyanite and pyrophyllite are commonly developed in the same horizons. Two general models have been suggested for the origin of these unusually aluminous, chloritoid-bearing assemblages within coarse-grained clastic sediments. The first, proposed by Wallmach and Meyer (1990), regards the formation of these aluminous layers as a function of prelithification surface weathering processes (i.e. metamorphism to an unusually aluminous palaeosol protolith). The alternative hypothesis, proposed by Phillips (1988) regarded these assemblages as being the result of metasomatism of chlorite and muscovite by an externally derived fluid at about the time of peak metamorphism. The chloritoid + pyrophyllite assemblages common in reef horizons are uncommon in regionally persistent metapelites. In such settings, muscovite + chlorite, muscovite + chlorite + chloritoid, and muscovite + chloritoid + pyrophyllite assemblages dominate and are attributed to fluid buffering along the muscovite breakdown curves in these originally more potassic rocks (Phillips, 1988). These bulk compositions had higher proportions of muscovite and lower porosities. Consequently, they buffered fluid composition more effectively during the alteration event. A rough paragenetic sequence from virtually

unaltered chlorite, to chloritoid, to pyrophyllite – by a process of Fe removal, acid metasomatism, and K mobility with increasing alteration – has been inferred (Phillips, 1988). Large-scale stratigraphic profiles documented by Fox and Winkler (1997) and Barnicoat *et al.* (1997) indicated that alteration zones of this type are continuous over distances of hundreds of kilometers around the northern rim of the Basin and are stratigraphically discordant. This appears to support a metasomatic alteration (as opposed to a surface weathering origin) for these aluminous assemblages.

The concept of a large-scale alteration system in the Witwatersrand Basin has been linked to the proposal that a significant quantity of gold was introduced into the Basin during high-temperature, syn- to post-peak alteration, and that the deposit should be regarded as a hydrothermal deposit (Phillips *et al.*, 1997a; Fox and Winkler, 1997; Barnicoat *et al.*, 1997). Barnicoat *et al.* (1997) and Phillips *et al.* (1997a) have documented complex paragenetic sequences for zones of alteration, with gold precipitation relatively late in the alteration sequences. However, these petrographic data are by no means a definitive argument for a hydrothermal origin for the gold. In particular, the paragenetic sequence proposed by Barnicoat *et al.* (1997) is very similar with respect to the relative timing and locations of gold precipitation to the model proposed by Robb and Meyer (1991; 1995) who interpreted this late gold precipitation in terms of remobilization of placer gold. In this model three stages of remobilization are proposed: (1) authigenic pyrite formation at 2500 Ma; (2) maturation of organic material and fluxing of hydrocarbon-bearing fluids through the Basin with the radiolytic fixation of bitumen around detrital uraninite; and (3) circulation of metamorphic fluids at the peak of metamorphism (~ 2.0 Ga) resulting in the widespread redistribution of gold and the formation of secondary sulphides. This model is similar to that of Frimmel *et al.* (1993) who proposed that fluid-rock interaction in reef horizons was on a relatively limited scale and that gold was not introduced into the Basin during metamorphism, but was rather remobilized over distances of centimetres. Frimmel (1994) categorised the fluid evolution in the Witwatersrand Basin into three major stages: (1) diagenesis; (2) burial associated with infiltration of fluids that interacted with the sediments of the Transvaal Supergroup; and (3) hydrothermal activity related to the Bushveld/Vredefort events. These views are supported by evidence from gold grain morphologies, which indicates that detrital gold grains clearly exist within certain reefs (Minter *et al.*, 1993). These pristine grains are rare, as might be expected given the metamorphic history of the Basin, but their presence does demonstrate a clastic input of gold into the Basin. Frimmel *et al.* (1993), working on metamorphic gold (i.e. the more common recrystallized, non-detrital gold grains) have documented evidence of gold geochemical variations between different reefs and different goldfields. They interpreted these data as evidence for clastic introduction of gold into the Basin from discrete and geochemically distinct source areas.

A Metamorphic Model for the Witwatersrand Basin

In contrast to the relatively advanced state of knowledge of the metamorphic pattern in the goldfields, the metamorphism of the remainder of the Witwatersrand Basin is poorly understood. Besides the goldfields, the only exposures of Witwatersrand rocks are to be found around the Vredefort Dome in the central part of the Witwatersrand Basin (Fig.1). Here, metamorphic grade increases with stratigraphic age towards the centre of the Dome. In the lower West Rand Group, exposed in the collar of the Dome, porphyroblastic cordierite, andalusite, biotite, garnet and/or staurolite metapelites indicate the attainment of mid-amphibolite facies conditions (Hall and Molengraaff, 1925; Nel, 1927; Bisschoff, 1982;

Gibson and Wallmach, 1995). Gibson and Wallmach (1995) estimated peak metamorphic temperatures of 570-600 °C at 4.0-4.5 kbar in these rocks. In the core of the Dome, garnet-, cordierite- and/or orthopyroxene-bearing metapelites, with or without migmatitic leucosomes, indicate the attainment of granulite facies conditions (850 °C to > 920 °C, ca. 5.0 kbar; Stevens *et al.*, 1997a). Until recently, the metamorphism in the collar of the Vredefort Dome was interpreted as a localised effect associated with the formation of the Dome, and its relationship to the metamorphism observed in the wider Basin was regarded as problematic (e.g., Phillips and Law, 1994; Frimmel, 1994). However, Gibson and Wallmach (1995) and Stevens *et al.* (1997a) demonstrated that the peak metamorphic assemblages in both the collar and the core predate the shock deformation linked to the formation of the Dome and have proposed that the metamorphism in both localities is linked to the same period of pre-Vredefort heating. Different ages have been suggested for the metamorphism in the collar supracrustals and the basement rocks (e.g., Bisschoff, 1982; Hart *et al.*, 1991). However, Gibson and Wallmach (1995) and Stevens *et al.* (1997a) proposed that on the grounds of: (1) similar, anticlockwise, pressure-temperature-path geometries for the collar and core metamorphism; (2) circumstantial evidence that both the medium-and high-grade metamorphism occurred within only a few tens of millions of years of the 2.02 Ga Vredefort Event; and (3) an absence of definitive geochronological data to the contrary, the high-temperature, low-pressure metamorphism (40-50°C/km) in both the core and collar rocks was the result of mantle heat addition to the crust and most probably resulted from a period of elevated craton - wide heat flow during the Bushveld Event.

This model (Gibson and Wallmach, 1995; Stevens *et al.*,1997a), which assumes a layer-cake heating of the Basin, and proposes that a substantial area of upper-greenschist to mid-amphibolite facies metamorphism exists within the centre of the Basin, has been used by Stevens *et al.* (1997b) to estimate the volume of metamorphic fluid produced from the West Rand Group. According to Stevens *et al.* (1997b), an average West Rand Group shale composition which attained 450 °C, would have liberated metamorphic fluid at a rate of 70 l/m^3 of rock. Metamorphism to approximately 600 °C, as occurred in the highest grade rocks exposed in the Vredefort collar would have resulted in an additional fluid production of 69 l/m^3. Given the model for the distribution of metamorphic grades within the Basin, this translates into a volume of $7{,}58\times10^{14}$ l/m^3 of aqueous fluid that was liberated from the West Rand Group shales. Stevens *et al.* (1997b) proposed this fluid as a significant agent of alteration and gold remobilization in the Central Rand Group.

Clearly, the development of an accurate basin-wide metamorphic model is important for evaluating the contribution of metamorphic fluids to the alteration and mineralisation history of the Witwatersrand Basin. The current model is based solely around data on the metamorphic history of rocks from the Vredefort Dome. Most previous studies on these rocks have proposed that the metamorphism in this area of the Witwatersrand Basin is unique to the Dome and is probably not related to regional metamorphism within the Basin. Thus, the predictions of metamorphic grade distribution made by Phillips *et al.* (1997a) and Stevens *et al.* (1997b) need to be tested by analysis of metamorphic material derived from the unexposed central portions of the Basin. In this study the metamorphism of West Rand Group shales intersected in boreholes from the central and southern portions of the Basin (Fig.1) is examined with the aim of furthering development of a Basin-wide metamorphic model.

Present Study

Cross sections through the Vredefort Dome, constrained by seismic and gravity data (Friese *et al.*, 1995; Henkel and Reimold, 1998), indicate that the rocks exposed in the southeastern sector of the Dome represent regions of the Basin that were originally more deeply buried than those sediments now exposed in the northwestern collar regions of the Dome. This relationship is the likely result of 1.2 to 1.0 Ga northwest-verging thrusting which has preferentially uplifted the southern, distal portions of the Basin relative to the central part (Friese *et al.*, 1995; Henkel and Reimold, 1998). As a result, the overturned to vertical rocks of the northern Vredefort collar have been removed by erosion in the southeastern sector of the Dome, resulting in the Witwatersrand suboutcrop in this region having a relatively shallow dip to the south (cf. Fig. 3b, Henkel and Reimold, 1998). Borehole NG1, located south of the Dome towards the southern limits of the present suboutcrop of Witwatersrand rocks (Fig. 1), intersects a near - complete succession of West Rand Group strata, down to a depth of 2,800m (Fig. 2). Borehole GH1 is located in the most southern portion of the Vredefort collar strata (Fig. 1) and intersects a limited succession of Government and Hospital Hill Subgroup lithologies, together with a large proportion of intrusive rocks (Fig. 2). The third borehole, VML1, intersects upper Jeppestown Subgroup strata (Fig. 2) to the east of the Vredefort Dome (Fig. 1).

PETROGRAPHY

Petrographic and bulk compositional data have been obtained from the Jeppestown, Government and Hospital Hill Subgroup intersections of all three boreholes. The most complete succession of West Rand Group rocks was sampled in borehole NG1. Forty two thin sections (Fig. 2) representing a broad sample of the stratigraphy were examined, and eighteen representative sections were finally chosen for more detailed petrographic analysis. Major-element geochemical data were collected for the 18 sample subset (Table 1). The data scatter widely on the standard AFM projection from muscovite (Fig. 3) and represent a range of considerably more ferruginous and less aluminous compositions than those detailed for metapelites exposed in the collar of the Vredefort Dome (Stevens *et al.*, 1997b). This trend on the AFM diagram is the result of variations in the Fe:Al ratio in the samples and is believed to reflect higher magnetite contents in the samples with the highest "F" values.

Petrographic analysis identified a stilpnomelane-bearing alteration assemblage as an important component of the sampled lithologies. This assemblage is particularly apparent in the borehole intersections to the south of the Vredefort Dome. A clear distinction can be made between a foliated metamorphic matrix assemblage and an alteration assemblage associated with fracture zones and veins. In general, the matrix assemblages are dominated by chlorite + quartz + muscovite. This assemblage constitutes the peak metamorphic assemblage in unaltered samples, with local variations to chlorite + quartz and chlorite + epidote + quartz in sediments of more mafic affinity. Local replacement of these assemblages to quartz + chlorite + stilpnomelane/ferrostilpnomelane + calcite + pyrite +/- epidote +/- chalcopyrite +/- garnet has occurred along fracture zones which appear to have been the focus of fluid ingress.

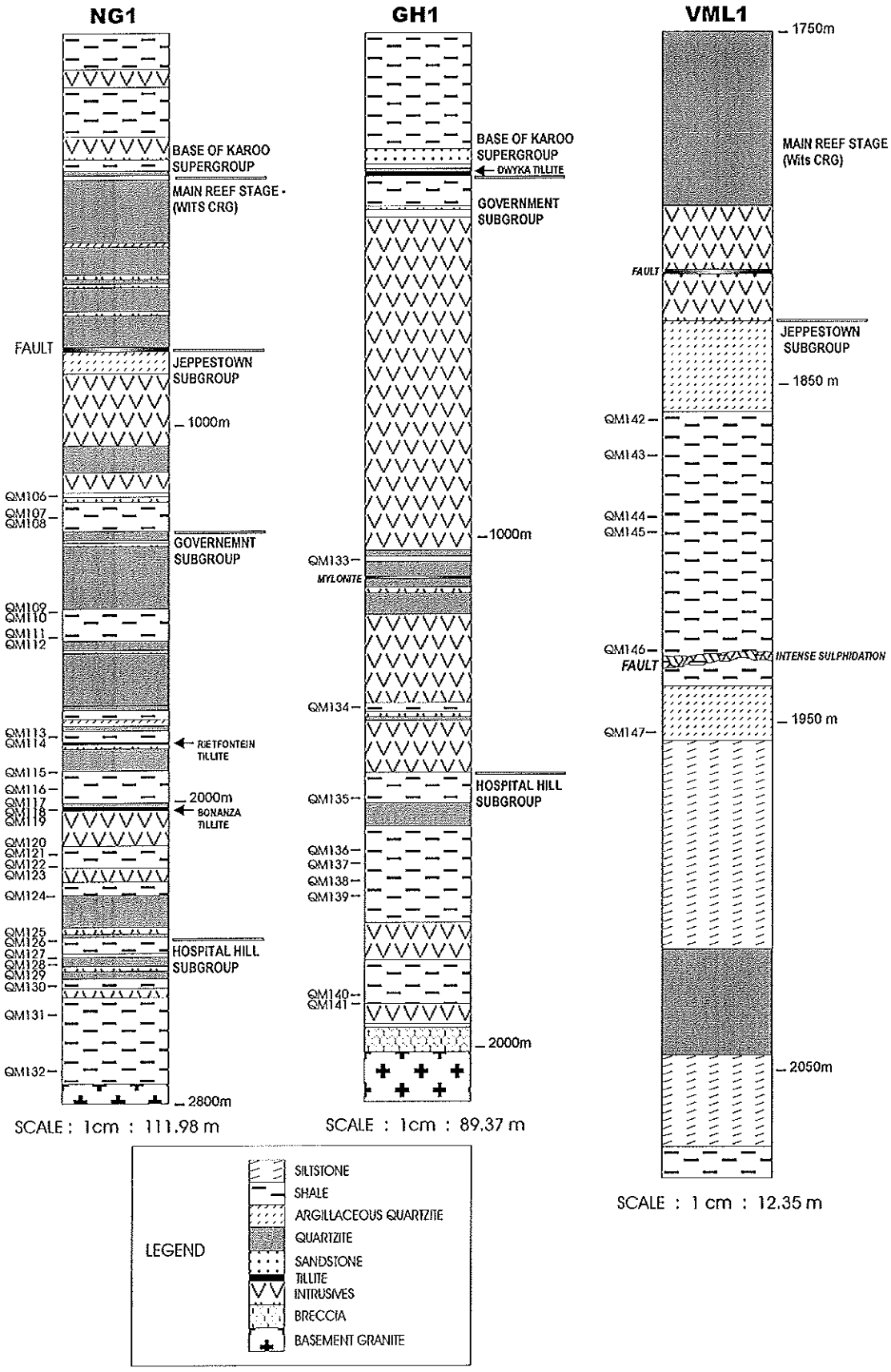

Figure 2: Borehole sections from NG1, GH1 and VML1, illustrating the position (in terms of stratigraphy and depth) of the samples examined.

Table 1: Major element compositions of samples from the Jeppestown, Government, and Hospital Hill Subgroups intersected in boreholes NG1, GH1 and VML1. The average West Rand Group shale (WGS) of Camden-Smith (1980) and representative metapelites from the Government and Hospital Hill Subgroups in the northern Vredefort collar (V40 and S6) from Stevens *et al.* (1997b) are also listed

	Ave.	Borehole NG1									
	WGS	QM107	QM108	QM110a	QM113b	QM117	QM118	QM120	QM121b	QM124	QM132
SiO_2	64.71	52.97	54.49	47.63	43.18	49.58	45.98	44.27	59.03	47.17	55.65
TiO_2	0.63	0.57	0.77	0.50	0.36	0.57	0.52	0.72	0.56	0.48	0.56
Al_2O_3	14.9	12.05	17.55	11.55	6.77	13.03	11.51	15.93	12.00	11.98	12.88
Fe_2O_3	12.49	24.57	13.85	30.51	20.04	24.62	27.2	25.05	17.98	28.49	20.32
MnO	0.00	0.14	0.10	0.09	0.52	1.13	3.49	2.15	0.99	0.31	1.32
MgO	4.76	4.08	4.98	3.84	3.55	3.58	3.36	4.58	4.06	4.89	2.79
CaO	0.45	0.68	0.92	0.54	11.84	2.75	3.26	0.76	0.83	0.28	1.35
Na_2O	0.00	0.00	0.31	0.00	0.04	0.00	0.00	0.00	0.68	0.00	0.00
K_2O	2.10	0.00	2.35	0.00	0.46	0.29	0.66	1.45	0.16	0.00	1.68
P_2O_5	0.00	0.08	0.19	0.05	0.05	0.16	0.13	0.05	0.05	0.21	0.09
LOI	NA	5.16	4.64	5.22	13.71	4.78	4.20	5.63	4.20	6.40	3.66
Total	100.00	100.33	100.16	99.94	100.53	100.50	100.32	100.59	100.55	100.21	100.32

	Borehole GH1						Borehole VML1		Stevens et al.	
	QM133	QM134	QM135b	QM136b	QM137	QM140b	QM143	QM145	S6	V40
SiO_2	56.6	36.4	49.96	43.00	57.72	43.26	42.21	50.59	61.18	57.31
TiO_2	0.75	0.37	0.43	0.53	0.53	0.20	0.63	0.61	0.62	0.54
Al_2O_3	19.19	6.61	8.50	11.86	11.66	2.09	12.03	12.42	19.38	18.92
Fe_2O_3	10.07	44.8	24.96	35.25	35.25	38.84	33.48	18.94	7.17	14.09
MnO	0.15	0.17	5.28	1.47	1.47	0.60	0.16	0.12	0.08	0.14
MgO	4.18	2.64	3.09	4.15	4.15	2.78	5.99	5.68	4.62	4.97
CaO	0.40	0.45	2.73	0.17	0.17	7.55	0.63	0.45	0.07	0.06
Na_2O	0.20	0.00	0.00	1.00	1.00	0.09	0.00	0.00	0.87	0.14
K_2O	3.76	0.03	1.57	1.23	1.23	0.49	0.15	0.5	3.01	2.82
P_2O_5	0.08	0.21	0.08	0.04	0.04	0.10	0.12	0.15	0.10	0.18
LOI	5.165	9.08	3.08	1.92	1.92	4.48	5.27	11.08	1.75	1.12
Total	100.53	100.78	99.69	100.62	100.62	100.49	100.68	100.55	98.84	99.99

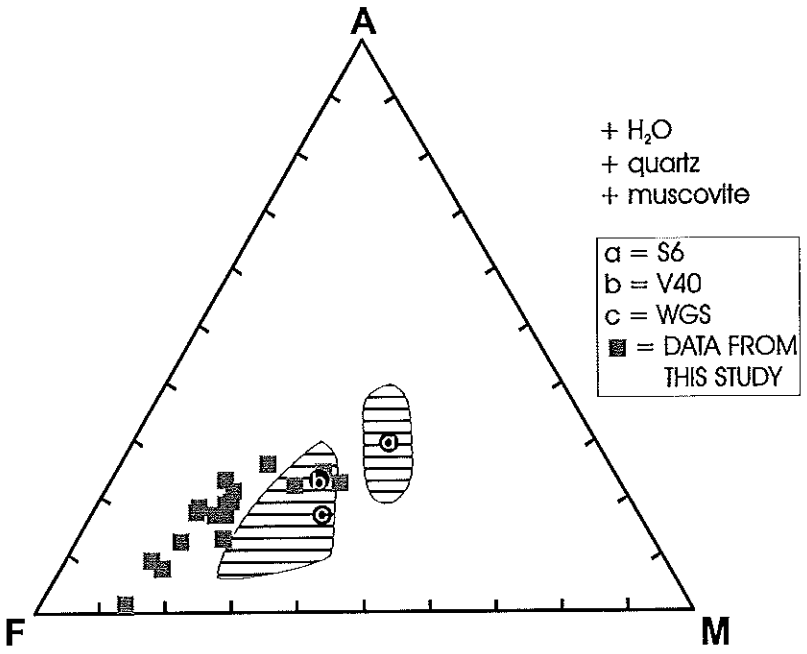

Figure 3: AFM projection from muscovite, quartz and water for the 18 bulk rock compositions determined in this study. The shaded fields represent the two groups of West Rand Group compositions identified by Stevens et al. (1997b). (a) and (b) represent what Stevens et al. (1997b) considered to be representative compositions of these two groups. Point (c) represents the average West Rand Group shale composition of Camden-Smith (1980).

Matrix Assemblages

Primary sedimentary layering, with alternation between argillaceous and more arenaceous (silty) interlayers, and soft-sediment deformation features are well preserved in some samples. The matrix assemblages vary only slightly throughout the sample set. Generally, chlorite constitutes the dominant phase and is associated with subordinate quartz, both detrital and metamorphic, and acicular muscovite. In more siliceous interlayers, large, acicular laths of muscovite, intergrown with chlorite, are developed as interstitial phases to primary quartz and plagioclase. The mineralogy of the cleaved matrix assemblages has been locally influenced by alteration processes in samples from close to alteration zones. This is illustrated by stilpnomelane, which occurs as a matrix phase in several samples, but is confined to samples, or areas within samples, that are adjacent to zones of alteration. These are interpreted as zones of less intense alteration, where the matrix fabric has been preserved, but where stilpnomelane has been produced.

Epidote is developed in the matrix assemblage in samples possessing bulk compositions of more mafic affinity and is a particularly abundant phase in samples QM113b and QM140b, which have CaO contents significantly higher than normal argillitic sediments (Table 1). In such samples, the matrix assemblage is epidote + chlorite + quartz.

Carbonaceous matter is an important matrix phase in some samples from both NG1 and GH1, where the shale matrix is massive and black in thin section. In these samples a fine grained intergrowth of carbonaceous material and magnetite is discernable in reflected light.

In other samples, the carbonaceous material is less concentrated and chlorite and muscovite can be identified. In many of these samples, finely laminated sedimentary bedding can be discerned and the carbonaceous material is regarded as primary. Pyrite occurs as a disseminated phase within the more carbonaceous zones of these samples. Table 2 summarizes the matrix assemblages identified from the entire sample set.

Table 2. Tabulated matrix assemblages for the sample suite from boreholes NG1, GH1 and VML1. Mineral abbreviations are from Kretz (1983)

SAMPLE No.	ASSEMBLAGE
QM106	CHL + MS + QTZ + STILP (ALTERED)
QM107	CHL + QTZ
QM108	CHL + MS + QTZ
QM109	CHL + QTZ + MS
QM110a	CHL + QTZ + CC
QM110b	CHL + QTZ + CC
QM111	CHL
QM112a	CHL + QTZ + STILP (ALTERED MATRIX
QM112b	+ FERRO STILP VEINS)
QM113a	CHL + CC + STILP (ALTERED MATRIX)
QM113b	
QM114	CHL + STILP (ALTERED MATRIX)
QM115a	QTZ + MS +/- CHL
QM115b	QTZ + MS +/- CHL
QM116a	QTZ + PL + LITHIC FRAGMENTS;
QM116b	INTERSTITIAL MS & CHL
QM117	CHL + QTZ + MS +/- EP (ASS. WITH ALTERATION)
QM120	CHL + PYRITE + GRT (ASS. WITH ALTERATION)
QM121a	CHL + QTZ + EP +/- PYRITE
QM121b	CHL + QTZ + EP +/- PYRITE
QM122	CHL + QTZ
QM123	CARBONACEOUS MATERIAL + QTZ +/- CHL
QM124	CHL + QTZ
QM125	QTZ + CHL + PYRITE IN CARBONACEOUS MATRIX
QM126	CHL + QTZ + GRN IN CARBONACEOUS MATRIX (ASS. WITH ALTERATION)
QM127	CHL +/- MS + GRT
QM128	CHL +/- MS IN CARBONACEOUS
QM129	MATRIX
QM130a	QTZ + CHL + MS + CARBONACEOUS
QM130b	MATERIAL + PYRITE + MAGNETITE
QM132	CHL + MS + QTZ +/- EPIDOTE
QM133	QTZ + MS
QM134	CARBONACEOUS MATRIX
QM135a	CHL + QTZ IN CARBONACEOUS MATRIX
QM135b	
QM136a	CHL + QTZ + CARBONACEOUS MATERIAL + GRT (ASS. WITH ALTERATION)
QM136b	QTZ + CHL + MS + PYRITE + CARBONACEOUS MATERIAL
QM137	TWO ZONES: FINE GRAINED CHL + QTZ & COARSER GRAINED CHL + MS + QTZ +/- EPIDOTE
QM138	CHL + MS + QTZ + EP
QM140a	CHL + EP + CC
QM140b	CARBONACEOUS MATRIX, TRANSITION INTO CHL + MS MATRIX
QM142	CHL + MS + QTZ +/- EP
QM143	CHL + MS + QTZ +/- EP
QM144	CHL + QTZ + MS
QM145	CHL
QM147	CHL + MS + QTZ + PYRITE +/- EP

Alteration Assemblages

The alteration assemblages are more complex than are the matrix assemblages of most samples. Alteration is commonly associated with zones of faulting and hydro-fracturing, with subsequent fluid ingress forming, in most cases, discreet, chlorite–rich veins (Fig. 4). Other minerals commonly associated with zones of alteration are pyrite, calcite, quartz, stilpnomelane, epidote and rarely, garnet. Stilpnomelane occurs in both acicular and platy forms and is intimately associated with pyrite mineralisation within veins and commonly overgrows both calcite and pyrite. Adjacent to these zones of marked alteration, the chlorite + muscovite matrix assemblage is altered to ferrostilpnomelane (the more Fe^{2+}- rich version of stilpnomelane) (Fig. 5).

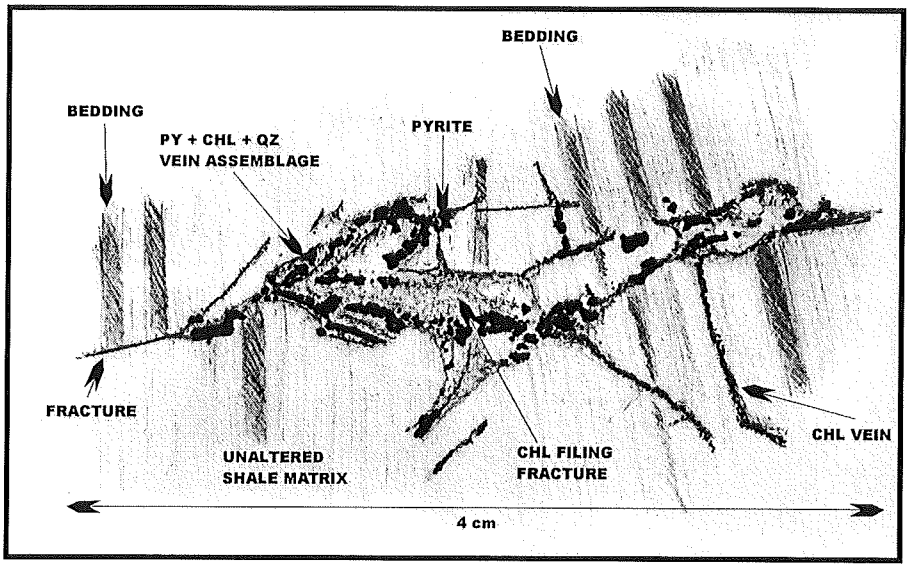

Figure 4: Line drawing of thin section QM107 illustrating the development of a quartz-chlorite-pyrite-dominated alteration assemblage related to fracturing and fluid ingress, which clearly cross-cuts the original sedimentary layering.

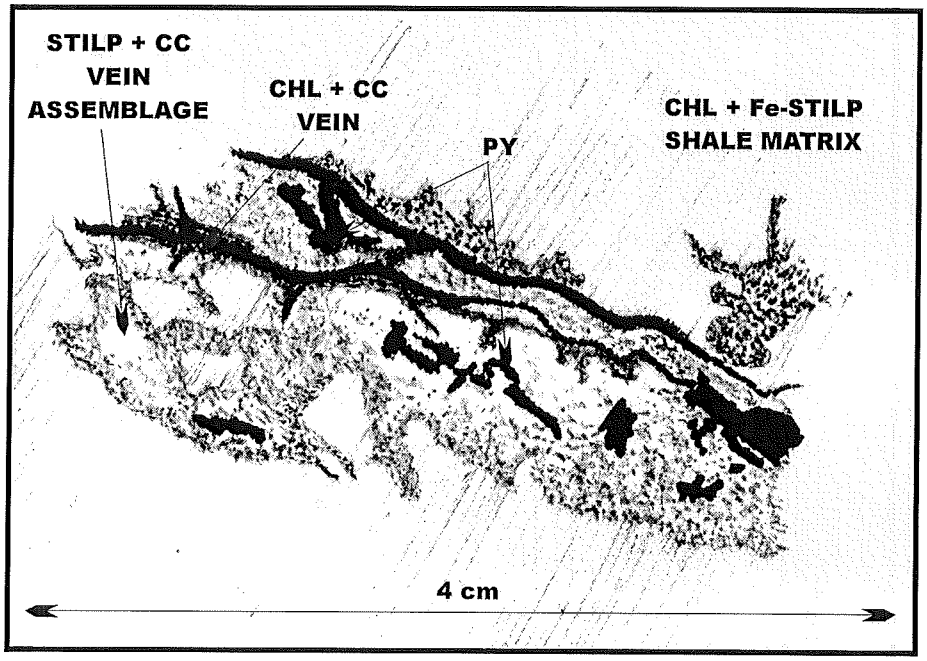

Figure 5: Line drawing of thin section QM106 illustrating the pervasive alteration of originally argillaceous sediment to a stilpnomelane/ferrostilpnomelane + pyrite-rich assemblage, associated with ingress of external derived fluid. Chlorite occurs in discrete veinlets within the altered groundmass.

Muscovite is absent from stilpnomelane-bearing areas. Consequently, stilpnomelane is interpreted to form via a reaction of the type: muscovite + chlorite = stilpnomelane. Attempts to balance this reaction using the mineral compositions measured in this study (Tables 3 and 4) failed, because the measured K/Al and (Fe + Mg)/Al ratios in the stilpnomelane require the production of an additional, more aluminous mineral than stilpnomelane in the products. No such mineral has been identified in this study. Al is typically regarded as relatively immobile in alteration and metasomatic processes. Consequently, large-scale mobility of K and Fe, and to a lesser degree Mg, are inferred in the alteration process in these samples. In Mn-rich samples garnet (Table 4) is commonly produced in association with the more typical alteration minerals. These garnet crystals are extremely fine grained and occur as nodular aggregates with poorly developed crystal faces. They do not appear completely isotropic in thin section, have high Mn and relatively high Ca contents (Table 4), and may contain a hydro-garnet component.

Sample QM122, from borehole NG1, documents remarkably well the details of the alteration episode (Fig. 6). Three zones of alteration can be identified within the sample: (1) essentially unaltered silicate matrix material, characterized by the general assemblage quartz + chlorite + muscovite, and containing small, disseminated pyrite grains; (2) a zone of more intense alteration, which is highly chloritised relative to the surrounding groundmass; and (3) a zone of intense alteration characterized by the association of relatively coarsely crystalline chlorite with garnet and pyrite. An interesting feature of this sample is a clear association of migrated and concentrated carbonaceous material with the most highly altered zones of the sample. These zones also contain disseminated pyrite and magnetite. It is clear that this alteration has been focussed along more permeable layers within the shale, with marked fluid flow, as indicated by the location of the carbonaceous material, exploiting lithological contacts. This phenomenon is also observed in sample QM136A (borehole GH1), where carbonaceous material, associated with pyrite, magnetite, chlorite and garnet, has been precipitated where fluid has migrated along the contact between a more siliceous sedimentary wedge within the largely argillitic rock mass.

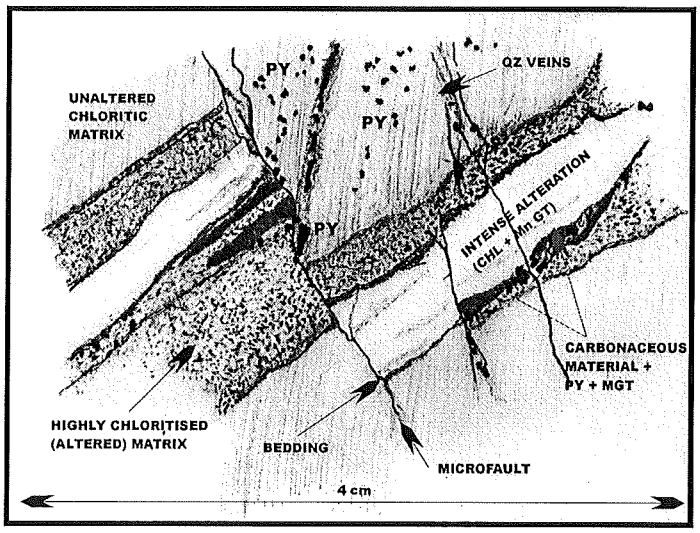

Figure 6: Line drawing of thin section QM122 showing the spatial relationship between different degrees of alteration related to fluid ingress along bedding planes. Carbonaceous material, together with pyrite and magnetite is concentrated along bedding surfaces.

Table 3: Average electron microprobe chlorite compositions from 11 samples analyzed. For samples which contain both vein or alteration (v) and matrix (m) chlorites the average compositions of the vein chlorites are listed in the second column for that sample

	Borehole NG1								
	QM106	QM110	QM110	QM113	QM117	QM117	QM120	QM120	QM124
n	6 m	3 m	1 v	4 v	2 m	5 v	6 m	7 v	3 v
SiO_2	24.15	23.69	25.26	24.64	23.95	24.27	24.05	23.35	23.22
TiO_2	0.04	0.03	0.04	0.06	0.00	0.05	0.03	0.09	0.08
Al_2O_3	18.01	19.29	19.11	18.88	20.00	19.62	19.30	19.86	18.26
Cr_2O_3	0.13	0.07	0.00	0.15	0.10	0.11	0.06	0.08	0.04
FeO	40.15	41.73	39.97	37.83	39.08	40.27	36.24	35.90	37.92
MnO	0.14	0.13	0.31	0.46	0.91	0.85	1.53	1.52	0.47
MgO	6.90	6.11	5.89	8.19	6.31	6.38	8.31	7.82	6.92
CaO	0.06	0.04	0.00	0.07	0.14	0.10	0.06	0.05	0.05
Na_2O	0.06	0.06	0.18	0.17	0.08	0.16	0.08	0.04	0.00
K_2O	0.04	0.03	0.04	0.03	0.02	0.01	0.03	0.01	0.05
Total	89.68	91.18	90.80	90.48	90.59	91.82	89.69	88.72	87.01
Si	5.38	5.22	5.57	5.37	5.28	5.29	5.28	5.19	5.32
Al	4.73	5.00	4.96	4.85	5.19	5.03	4.99	5.20	4.92
Ti	0.01	0.00	0.01	0.01	0.00	0.01	0.00	0.01	0.01
Fe^{3+}	0.49	0.54	0.00	0.43	0.26	0.42	0.45	0.38	0.41
Fe	7.00	7.14	7.37	6.47	6.95	6.92	6.21	6.30	6.85
Cr	0.02	0.01	0.00	0.03	0.02	0.02	0.01	0.01	0.01
Mn	0.03	0.02	0.06	0.09	0.17	0.16	0.28	0.29	0.09
Mg	2.29	2.01	1.94	2.66	2.07	2.07	2.72	2.59	2.36
Ca	0.01	0.01	0.00	0.02	0.03	0.02	0.01	0.01	0.01
Na	0.03	0.03	0.08	0.07	0.03	0.07	0.03	0.02	0.00
K	0.01	0.01	0.01	0.01	0.01	0.00	0.01	0.00	0.01
Cations	20.00	19.99	19.98	20.01	20.01	20.01	19.99	20.00	19.99
$^{[4]}Al$	2.62	2.78	2.43	2.63	2.72	2.71	2.72	2.81	2.68
Xfe	0.75	0.78	0.79	0.71	0.77	0.77	0.70	0.71	0.74
T (°C)	308	331	234	307	311	294	321	322	298

	Borehole GH1		Borehole VML1			
	QM136	QM137	QM142	QM145	QM145	QM147
n	5 m	9 m	9 m	9 m	1 v	5 m
SiO_2	25.74	24.25	24.55	24.57	24.27	24.76
TiO_2	0.07	0.10	0.07	0.06	0.03	0.04
Al_2O_3	19.93	19.65	20.45	20.48	20.60	19.99
Cr_2O_3	0.12	0.12	0.26	0.07	0.00	0.12
FeO	25.78	30.65	31.96	34.93	36.35	31.99
MnO	3.55	2.65	0.17	0.15	0.27	0.22
MgO	13.99	10.56	10.68	9.75	9.45	10.94
CaO	0.06	0.05	0.05	0.05	0.06	0.02
Na_2O	0.02	0.04	0.02	0.07	0.07	0.06
K_2O	0.04	0.04	0.02	0.02	0.00	0.01
Total	89.30	88.11	88.23	90.15	91.10	88.15
Si	5.42	5.31	5.35	5.29	5.19	5.39
Al	4.94	5.07	5.25	5.19	5.19	5.13
Ti	0.01	0.02	0.01	0.01	0.00	0.01
Fe^{3+}	0.17	0.28	0.00	0.21	0.43	0.07
Fe	4.38	5.33	5.82	6.08	6.08	5.75
Cr	0.02	0.02	0.05	0.01	0.00	0.02
Mn	0.63	0.49	0.03	0.03	0.05	0.04
Mg	4.39	3.45	3.47	3.13	3.01	3.55
Ca	0.01	0.01	0.01	0.01	0.01	0.00
Na	0.01	0.02	0.01	0.03	0.03	0.02
K	0.01	0.01	0.01	0.01	0.00	0.00
Cations	19.99	20.01	20.00	20.00	19.99	19.98
$^{[4]}Al$	2.58	2.69	2.65	2.71	2.81	2.61
Xfe	0.50	0.61	0.63	0.66	0.67	0.62
T (°C)	294	299	278	298	331	278

Table 4: Representative electron microprobe garnet and stilpnomelane compositions from this study. The garnet mineral formula has been calculated using 24 oxygen, the formulae of stilpnomelanes have been calculated assuming 8 Si

mineral	QM106 Stilp.	QM106 Ferrostilp.	QM120 Garnet
SiO_2	44.30	45.37	36.44
TiO_2	0.00	0.00	0.16
Al_2O_3	5.35	5.60	19.43
Cr_2O_3	0.00	0.00	0.10
FeO	33.40	35.73	14.64
MnO	0.48	0.23	25.72
MgO	3.99	4.23	0.58
CaO	0.00	0.00	2.32
Na_2O	1.08	0.40	0.00
K_2O	3.35	2.54	0.00
Total	91.95	94.10	99.39
Si	8.00	8.00	6.03
Al	1.14	1.16	3.79
Ti	0.00	0.00	0.02
Fe^{3+}			
Fe	5.05*	5.27*	2.03
Cr	0.00	0.00	0.01
Mn	0.07	0.03	3.61
Mg	1.08	1.11	0.14
Ca	0.00	0.00	0.41
Na	0.38	0.14	0.00
K	0.77	0.57	0.00
Cations	16.49	16.28	16.04

QUANTIFYING THE METAMORPHISM AND ALTERATION OVERPRINT

The stilpnomelane-producing reaction is likely to be a prograde devolatilization reaction, as stilpnomelane typically contains significantly less H_2O than chlorite. The fact that stilpnomelane is confined to alteration zones indicates that the production of this phase is not only a function of metamorphic grade, but is predominantly a function of fluid ingress. The fact that muscovite + chlorite breakdown has produced stilpnomelane in preference to the more typical biotite, probably indicates that the reaction occurred at a temperature below biotite stability. Stilpnomelane in the alteration veins is deep red, a characteristic of the Fe^{3+}-rich variety of the mineral. In contrast, in areas of less intense alteration, where this mineral occurs in the matrix, it is pale-green, typical of the Fe^{2+}-rich variety, ferrostilpnomelane. This indicates that the metasomatising fluids were probably relatively oxidising and is supported by the association of magnetite + pyrite in several of the altered samples. The presence of calcite and pyrite in the alteration zones further indicates that Ca and S, in addition to Fe and K, were mobile in the fluid phase. Small quantities (~100g) of 13 altered samples from this study were assayed for Ag and Au (analysis conducted by Bergström and Bakker Laboratories in Johannesburg). Several samples contained gold to a concentration of approximately 0.5 ppm, indicating that on this small scale, fluid infiltration introduced gold into the shales. The assayed samples are typified by the association of carbonaceous matter, magnetite and pyrite and, have obviously been enriched with respect to gold to values exceeding normal background for regionally persistent Witwatersrand shales. Phillips (1987b) carried out a survey of 140 shale samples and identified regionally persistent shales away from reef horizons zones displayed values of less than 5 ppb Au. Samples analysed during this study are thus clearly anomalous and the high Au values are interpreted as related to late-stage introduction of gold together with pyrite and the carbonaceous material.

The metamorphic assemblage chlorite + muscovite + quartz constrains the conditions of metamorphism to below those of the reaction Mu + Chl = Bt + And + Qtz + H_2O, which commences at a temperature of approximately 400°C within the pressure range 2 to 4 kbar (Ferry, 1984). The chlorite + quartz + epidote assemblages developed in the Ca-rich shales are also consistent with equilibration under lower greenschist facies conditions. The precise metamorphic conditions represented by the stilpnomelane-producing reaction, as well as those represented by the metamorphic peak recorded by the matrix assemblages, are difficult to quantify accurately because of the high variance of the matrix assemblages, a lack of information about the thermal stability of stilpnomelane, and the obviously metasomatic character of the assemblages in the zones of alteration. Chlorite thermometry has been used effectively in studies of metamorphic temperatures in the goldfields (e.g. Frimmel, 1997) and, given the limitations of the sample material, appears to be the best technique for attempting to quantify metamorphic temperatures in this study as well.

Chlorite Thermometry

Chlorite compositions from 11 samples were obtained by electron microprobe analysis using the Cameca instrument at the Geology Department at the Rand Afrikaans University. During the analyses the accelerating voltage was 15 kV, the beam current was 40 ηA, the analysis spot size was 1 to 2 μm, and the counting time was 80 seconds. For calibration of the instrument natural mineral standards were used, and the ZAF correction procedure was employed. All the chlorite analyses were recalculated on the basis of 20 oxygens and 16 monovalent anions (OH, Cl and F). Average matrix and vein chlorite compositions in the 11 samples are presented in Table 3. Individual analyses are plotted on a Fe^{2+} + Fe^{3+} versus Si content diagram (Figure 7). The Fe^{3+} contents were determined according to Droop (1987), where cation totals in excess of 20 (in chlorite) are attributed to the presence of Fe^{3+} in the mineral structure.

The chlorite compositions determined in this study plot very close to that of the clinochlore end-member (Robinson *et al.*, 1993) on a plot of total interlayer cations (Si + Al + Cr + Fe + Mg + Mn) versus Al (Fig. 8a). In Figure 8b the data from two studies which documented chlorite compositions in the goldfields (Frimmel, 1997; Phillips *et al.*, 1997b) have been plotted on the same diagram for comparison. The data from the present study represent a much more restricted compositional range than determined in previous studies and plot closer to the clinochlore end-member than those of Frimmel (1997), but overlap with the most clinochlore-rich compositions of Phillips *et al.* (1997b). The matrix and vein chlorite populations from this study are indistinguishable in the plots of Figure 7 and 8a. The main compositional variation in the current data set is a function of variations in Mg# and Mn content. This is illustrated on Figure 7, where the Si contents of all the chlorites from the present study fall within the range from 5.2 to 5.6. Fe contents of the chlorites are highest in samples from borehole NG1, they are intermediate in samples from borehole VML1, and are lowest in samples from borehole GH1. These differences are a consequence of variation in bulk rock composition, with lower total Fe in chlorite reflecting more Mg-rich compositions in the case of the VML1 samples and higher Mn-content in the case of GH1 samples.

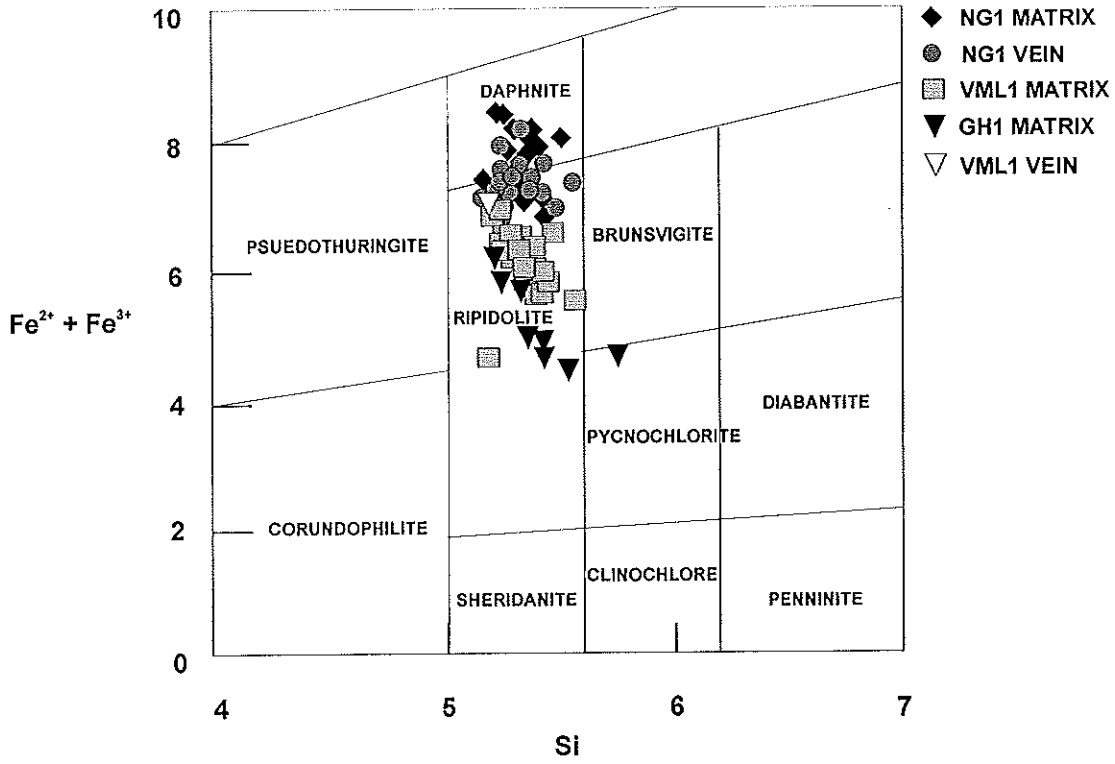

Figure 7: Individual chlorite compositions from 76 microprobe analyses.

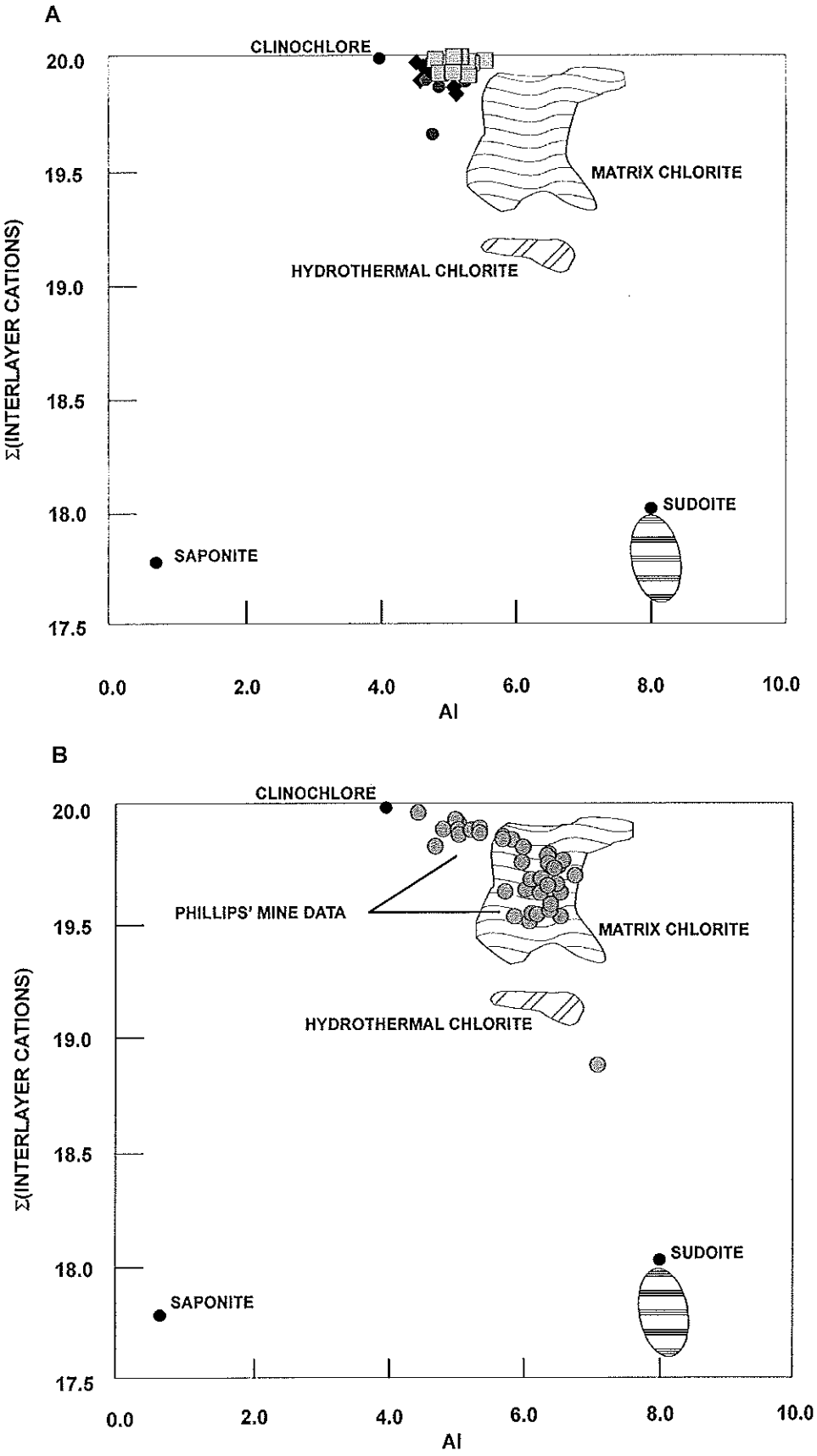

Figure 8: (8a) Comparison between the chlorite compositions determined by Frimmel (1997) from the goldfields (shaded fields), and the data from this study (symbols as for Fig. 7). (8b) Comparison between the chlorite compositions determined by Frimmel (1997) from the goldfields (shaded fields), and the data from Phillips et al. (1997b) (shaded points).

Cathelineau (1988) demonstrated that the $^{[4]}$Al content of chlorite produced through hydrothermal alteration of andesite increases as a function of increasing temperature of formation and could be used as a geothermometer. The application of the chlorite thermometer is problematic, because, as discussed by Jiang *et al.* (1994), chlorite octahedral vacancies and, thus, $^{[4]}$Al content can be the result of submicroscopic inclusions or interlayers within chlorite. They suggested that such contaminated chlorites will typically have variable Ca + Na + K contents, whereas pure chlorites will have little or no Ca + Na + K. Frimmel (1997) found that chlorites from the goldfields of the Witwatersrand Basin, with a total Ca + alkalis content < 0.2 yielded results that were considered a reliable indication of equilibration temperature. The study of Frimmel (1997) also evaluated the suitability of three different calibrations of the chlorite geothermometer for Witwatersrand compositions (i.e. Cathelineau, 1988; Kranidiotis and MacLean, 1987; Zang and Fyfe,1995).

Frimmel (1997) concluded, on the basis of a comparison of his data with sudoite phase stability data and chlorite-chloritoid Fe:Mg partitioning thermometry, that the Zang and Fyfe (1995) calibration: T (°C) = 17.5 + 106.2 [$^{[4]}$Al - 0.88(X_{Fe} - 0.34)], represents the most consistently reliable estimation of chlorite equilibration temperatures in common Witwatersrand compositions. This thermometer has been applied to the chlorite compositions obtained in the present study (Table 3), as well as to the chlorite composition data published by Phillips *et al.* (1997b) (Table 5).

The data for matrix chlorites from this study indicate an average metamorphic peak temperature of 318 ± 13 °C in borehole NG1, 297 ± 3 °C in borehole GH1 and 285 ± 13 °C in borehole VML 1. Average chlorite thermometry temperatures from alteration zones generally fall within 15 °C of the relevant average matrix chlorite value. In borehole NG1, where samples were collected from over 1000m of core, the average temperatures increased only slightly with depth. Insufficient data exist to attempt to accurately fit a geotherm; however, the existing data do not support the existence of extremely high geotherms in the region of 50 °C/km as has been suggested by Gibson and Wallmach (1995). The temperature uncertainty associated with chlorite thermometry is considered to be in the range of 25 °C (Zang and Fyfe, 1995). Within this error level, there is no discernable difference in the temperature of equilibration between the vein and matrix chlorites from most samples in this study. Thus, the chlorite thermometry, combined with the petrographic observation that stilpnomelane, the highest grade metamorphic mineral in the samples, is confined to zones of alteration, suggests that alteration occurred close to the peak of metamorphism.

Table 5: Average electron microprobe chlorite compositions from various Witwatersrand goldfields (after Phillips *et al.*, 1997b)

	Beatrix	Blyvoor	Drief'tein	Mariev'le	Vredef'rt	Welkom	W Rand	W Rand
n	7	8	6	4	2	5	3	8
SiO_2	24.44	24.63	23.28	23.72	25.29	23.86	25.15	26.25
Al_2O_3	24.13	24.95	25.88	23.92	23.98	25.87	27.63	20.64
Cr_2O_3	0.30	0.07	0.25	0.31	0.20	0.00	0.09	0.30
FeO	25.59	25.92	24.90	26.17	21.06	28.08	15.50	20.76
MnO	0.23	0.14	0.11	0.23	0.23	0.44	0.09	0.31
MgO	11.11	10.87	11.97	11.49	16.69	8.91	18.31	17.60
Total	85.80	86.59	86.48	85.82	87.44	87.16	86.77	85.85
Si	5.26	5.25	4.96	5.14	5.21	5.11	5.04	5.52
Al	6.12	6.25	6.51	6.09	5.82	6.53	6.53	5.11
Fe^{3+}	0.00	0.00	0.00	0.00	0.00	0.00	0.00	0.00
Fe	4.61	4.63	4.43	4.75	3.63	5.04	2.60	3.67
Cr	0.05	0.01	0.04	0.05	0.03	0.00	0.01	0.05
Mn	0.04	0.03	0.02	0.04	0.04	0.08	0.01	0.05
Mg	3.57	3.44	3.80	3.71	5.13	2.84	5.47	5.50
Cations	19.65	19.61	19.76	19.78	19.86	19.61	19.67	19.90
Al^4	2.74	2.75	3.04	2.86	2.79	2.89	2.96	2.49
Xfe	0.56	0.57	0.54	0.56	0.42	0.64	0.32	0.40
T (°C)	288	288	322	301	307	296	333	276

DISCUSSION

The findings of the petrographic and chlorite thermometry study may be summarized as follows:

- A metamorphic matrix assemblage exists which reflects the generally lower greenschist facies peak metamorphic conditions and bulk compositional variations within the samples.

- The metamorphic matrix assemblage is locally altered in response to fluid infiltration along sedimentary boundaries, fracture systems and fault planes to an assemblage commonly characterized by chlorite + ferrostilpnomelane/stilpnomelane + calcite + pyrite ± magnetite ± carbonaceous material. Clearly, the fluid that interacted with the country rock was in disequilibrium with the matrix assemblage, and induced the reaction of chlorite and muscovite to form stilpnomelane, with muscovite being preferentially consumed during the reaction as a result of its low concentration within the original matrix assemblage. This process involved substantial K and Fe metasomatism, with Mg, Ca and S also being mobile elements. During this process the alteration zones were also enriched in gold to a low level.

- The alteration event seems to have occurred at close to the peak of metamorphism as fluid influx appears to have induced breakdown of chlorite and muscovite to form ferrostilpnomelane and a second generation of chlorite through a prograde devolatilization reaction.

The data presented in this study place important constraints on a more complete basin-wide metamorphic model. Previous studies (e.g., Stevens *et al.*, 1997b) suggested a central region of upper-greenschist to lower-amphibolite-facies metamorphism within the Witwatersrand Basin. This model is based largely on the conclusion by Gibson and Wallmach (1995) that the peak amphibolite facies metamorphic event recorded by lower Witwatersrand strata in the collar of the Vredefort Dome predates the formation of the Dome and is thus

unrelated to the Dome-forming process. The data presented in this study suggest that these previous estimates of the metamorphic facies distribution within central portions of the Basin need to be revised and also have important implications for the origin of the high-grade metamorphism in the Vredefort collar.

Figure 9a illustrates the metamorphic facies distribution within the Basin as constrained by published data on the metamorphic grade within the goldfields, the exposed sections of the Vredefort collar, and the data from this study. Our findings clearly indicate lower-greenschist-facies grades of metamorphism in all three of the boreholes examined. Furthermore, while the accuracy of chlorite thermometry data may be debated in terms of its measure of absolute temperature, the comparison of the chlorite thermometry from this study with that from similar horizons in the goldfields (Table 5, and Frimmel, 1997), suggests that metamorphic grades in our samples and those along the current northern Basin margin are very similar. This may be the case for much of the Basin. This, coupled with the fact that the material currently exposed at surface and in boreholes is derived from depths ranging over several kilometers, must imply a relatively low thermal gradient throughout the Witwatersrand Supergroup during its metamorphic peak, which is generally considered to have occurred at approximately 2.0 Ga.

Borehole GH1 is located within the southern collar of the Vredefort Dome, yet the metamorphic grade in these samples is generally indistinguishable from that in boreholes VML1 and NG1. This observation suggests that the distribution of higher grade rocks (mid–amphibolite facies) in the northwestern portions of the collar strata of the Vredefort Dome are more localized than claimed by recent studies of Gibson and Wallmach (1995) and Stevens *et al.* (1997a), who attributed metamorphism in the Vredefort Structure to the same thermal perturbation (crustal underplating) responsible for the regional greenschist facies metamorphism developed throughout the Witwatersrand goldfields. This model requires a widespread high-grade metamorphic zone within the central portions of the Witwatersrand Basin, which is clearly not supported by the data of the present study. These findings agree with those of Bisschoff (1982), who noted a decrease in metamorphic grade both east and west of the area of high-grade metamorphism centred in the northwestern sector of the Vredefort collar, and imply a heat source other than a high regional geothermal gradient. Figure 9b represents a proposed distribution of metamorphic grades within the Witwatersrand Basin. The findings of this study have the following important implications:

- Previous metamorphic fluid production estimates, based on the existence of a regional zone of amphibolite facies metamorphism, are likely to be unduly high. Stevens *et al.* (1997b) calculated fluid production from an average West Rand Group shale and showed that the first major metamorphic fluid-producing reaction would be the production of biotite. Metamorphic fluid production from the rocks examined in this study would have been extremely limited.

- The origin of the amphibolite facies metamorphism in the northwestern Vredefort collar remains poorly understood (cf Reimold and Gibson, 1996). Clearly, as discussed by Gibson and Wallmach (1995), the highest grade rocks do not correlate with proximity to the alkali granites intruded into this area, which have been inferred as a heat source by previous workers, yet regional heating also appears unlikely. However, understanding the origin of this metamorphism and constraining its spatial extent remain major challenges to our understanding of the evolution of the Witwatersrand Basin.

- The alteration systems documented in the area of reef horizons in the Witwatersrand goldfields are difficult to study due to their scale. The issue of gold introduction into the Basin during the alteration process remains contentious. In the relatively distal shales examined in this study alteration zones that are similar to those inferred for the goldfields, in terms of the timing of alteration and the nature of the metasomatism, are developed on a much smaller scale. These zones are undoubtedly associated with gold introduction into rocks which formerly could not have been auriferous sediments.

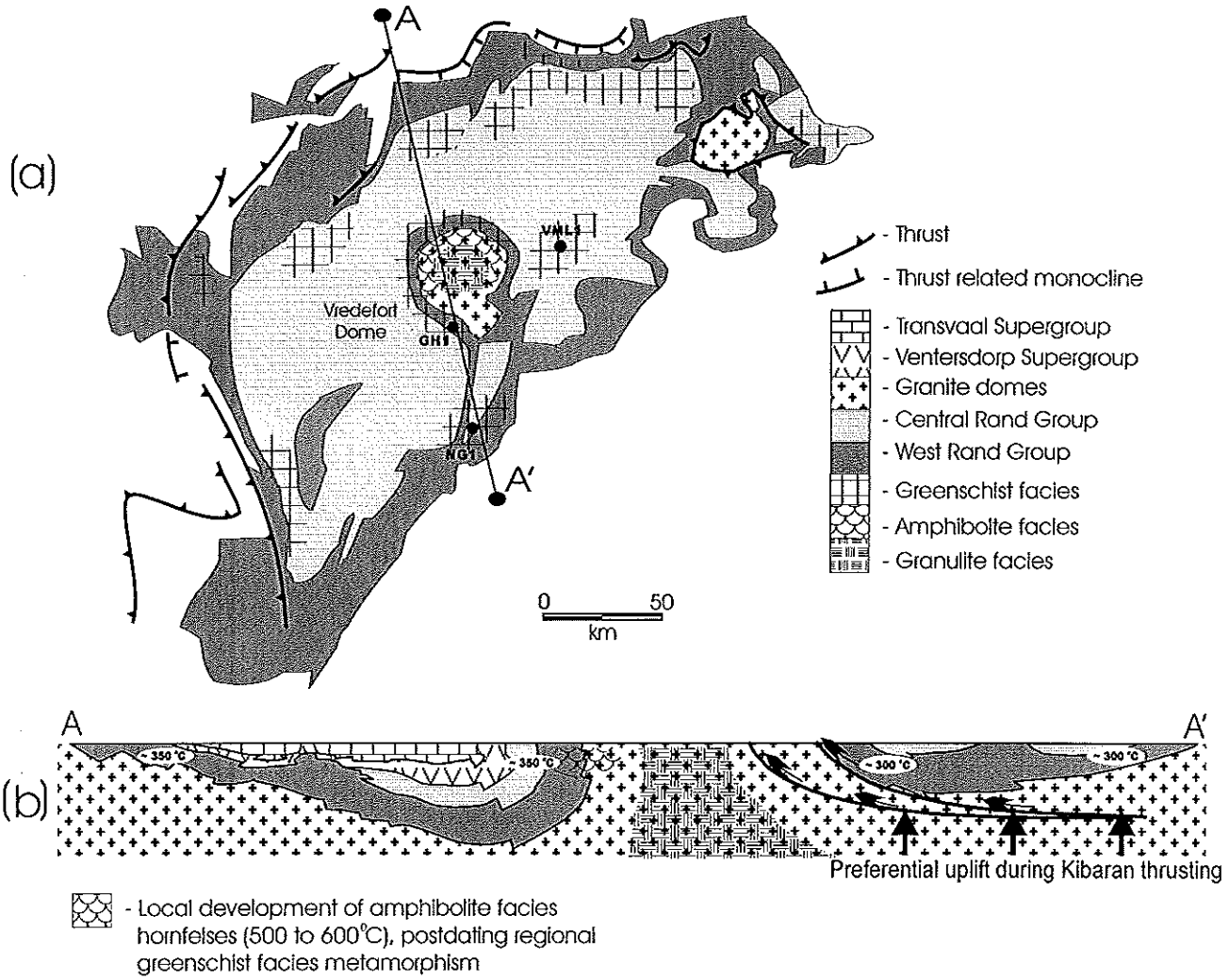

Figure 9: (9a) A simplified geological map of the Witwatersrand Basin and Vredefort Dome, illustrating the metamorphic facies distribution from previously published data, together with new data from this study. Note that West Rand Group strata in the southern portions of the Vredefort collar are at lower greenschist facies grade of metamorphism. (9b) Cross section A–A', illustrating a geophysically constrained section through the present-day Witwatersrand Basin (after Friese et al., 1995; Henkel and Reimold, 1998). In this section the proposed limited extent of the high-grade metamorphism in the northwestern collar of the Vredefort Dome is illustrated along with the proposed 300 to 350 °C lower greenschist facies metamorphism for much of the remainder of the Basin. The exact dimensions of the high grade zone are not well known at present, but they clearly do not include the southern collar. The granulites exposed in the core of the Dome represent a metamorphic terrane formed prior Witwatersrand sedimentation.

oOo

ACKNOWLEDGEMENTS

Access to borehole material and sample preparation by Anglo American Prospecting Services is gratefully acknowledged. In particular, we wish to thank Russell Dell for assisting with logistics. Research funding by the Foundation for Research Development is also gratefully acknowledged. Nellie Day is thanked for assistance with the microprobe analyses. The authors also wish to thank their colleagues at the University of the Witwatersrand, Johannesburg, who continue to provide interesting discussion on Witwatersrand and Vredefort issues. Carl Anhaeusser, Laurence Robb, Roger Gibson and Uwe Reimold are thanked for constructive reviews of the manuscript.

REFERENCES

Barnicoat, A.C., Henderson, I.H.C., Knipe, R.J., Yardley, B.W.D., Napier, R.W., Fox, N.P.C., Kenyon, A.K., Munting, D.J., Strydom, D., Winkler, K.S., Lawrence, S.R., and Cornford, C., 1997. Hydrothermal gold mineralization in the Witwatersrand basin. *Nature*, **386**, 820–824.

Bisschoff, A.A., 1982. Thermal metamorphism of the Vredefort Dome. *Transactions of the Geological Society of South Africa,* **85**, 45–57.

Camden–Smith, P.M., 1980. *The sedimentology, geochemistry and diagenesis of West Rand Group sediments in the Heidelberg area, Transvaal.* MSc. Thesis (unpubl.), University of the Witwatersrand, Johannesburg, 334 pp.

Cathelineau, M., 1988. Cation site occupancy in chlorites and illites as a function of temperature. *Clay Minerals*, **23**, 471-485.

Droop, G.T.R., 1987. A general equation for estimating Fe^{3+} concentrations in ferromagnesian silicates and oxides from microprobe analyses, using stoichiometric criteria. *Mineralogical Magazine,* **51**, 431-435.

Ferry, J.M., 1984. A biotite isograd in south-central Maine, USA: mineral reactions, fluid transfer and heat transfer. *Journal of Petrology*, **25**, 871–893.

Fox, N.P.C. and Winkler, K.S., 1997. Hydrothermal alteration of the Witwatersrand Basin. *In*: Hendry, J.P., Carey, P.F., Parnell, J., Ruffel, A.H. and Worden, R.H. (Eds.), *Fluid Migration and Interaction in Sedimentary Basins and Orogenic Belts. Geofluids II '97. Contributions to the 2nd International Conference on Fluid Evolution.* 440-443.

Friese, A.E.W., Charlesworth, E.G. and McCarthy, T.S., 1995. Tectonic processes within the Kaapvaal Craton during the Kibaran (Grenville) orogeny: Structural, geophysical and isotopic constraints from the Witwatersrand Basin and environs. *Information Circular Economic Geology Research Unit*, University of the Witwatersrand, Johannesburg, **292**, 67pp.

Frimmel, H. E., 1994. Metamorphism of Witwatersrand gold. *Exploration and Mining Geology,* **3**, 357–370.

Frimmel, H. E., 1997. Chlorite thermometry in the Witwatersrand Basin: Constraints on the Palaeoproterozoic Geotherm in the Kaapvaal Craton, South Africa. *Journal of Geology*, **105**, 601–615.

Frimmel, H. E., Le Roux, A.P., Knight, J. and Minter, W.E.L., 1993. A case study of the post depositional alteration of the Witwatersrand Basal Reef gold placer. *Economic Geology*, **88**, 249–265.

Gibson, R.L. and Wallmach, T., 1995. Low pressure – high temperature metamorphism in the Vredefort Dome, South Africa: anticlockwise pressure – temperature path followed by rapid decompression. *Geological Journal,* **30**, 319–331.

Hall, A.J. and Molengraaff, G.A.F., 1925. The Vredefort Mountain Land in the Southern Transvaal and the Northern Orange Free State. *Verhandeling van die Akademie. van Wetenskap. Sect..*, **2**, 24, 183pp.

Hart, R.J., Nicolaysen, L.O. and Gale, N.H., 1981. Radioelement concentrations in the deep profile through Precambrian basement of the Vredefort Structure. *Journal of Geophysical Research*, **86**, 10639 –10652.

Henkel, H. and Reimold, W.U., 1993. Integrated geophysical modelling of a giant, complex impact structure: anatomy of the Vredefort Structure, South Africa. *Tectonophysics*, **287**, 1–20.

Jiang, W.T., Peacor, D.R. and Buseck, P.R., 1994. Chlorite geothermometry – contamination and apparent octahedral vacancies. *Clay Minerals*, **42**, 593-605.

Kranidiotis, P. and Maclean, W.H., 1987. Systematics of chlorite alteration at the Phelps Dodge massive sulfide deposit, Matagami, Quebec. *Economic Geology*, **82**, 1898–1911.

Kretz, R., 1983. Symbols for rock forming minerals. *American Mineralogist*, **68**, 277-279.

Minter, W.E.L., Goedhart, M., Knight, J. and Frimmel, H.E., 1993. Morphology of Witwatersrand gold grains from the Basal Reef: Evidence for the detrital origin. *Economic Geology*, **88**, 237-265.

Nel, L.T., 1927. The geology of the country around Vredefort. *Special Publication of the Geological Survey of South Africa*, **6**, 134pp.

Phillips, G.N., 1987a. Metamorphism of the Witwatersrand goldfields: Conditions during peak metamorphism. *Journal of metamorphic Geology*, **5**, 307-322.

Phillips, G.N., 1987b. Anomalous gold in Witwatersrand shales. *Economic Geology*, **82**, 2179 –2186.

Phillips, G.N., 1988. Widespread fluid infiltration during metamorphism of the Witwatersrand goldfields: generation of chloritoid and pyrophyllite. *Journal of metamorphic Geology,* **6**, 311–332.

Phillips, G.N. and Myers, R.E., 1989. The Witwatersrand goldfileds II: An origin for Witwatersrand gold during metamorphism and associated alteration. *Economic Geology Monograph 6*, 598–608.

Phillips, G.N. and Law, J.D.M., 1994. Metamorphism of the Witwatersrand goldfields: a review. *Ore Geology Reviews,* **9**, 1–31.

Phillips, G.N., Law, J.D.M. and Stevens, G., 1997a. Alteration, heat and Witwatersrand Gold: 111 years after Harrison and Langlaagte. *South African Journal of Geology*, **100**, 377-392.

Phillips, G.N., Zhou, T. and Powell, R., 1997b. Metamorphic temperature variations among Witwatersrand goldfields: evidence from the pyrophyllite – chloritoid – chlorite mineral assemblage. *S. Afr. J. Geol.*, **100**, 393-404.

Reimold, W.U. and Gibson, R.L., 1996. Geology and evolution of the Vredefort Impact Structure, South Africa. *Journal of African Earth Sciences*, **23**, 125-162.

Reimold, W.U., Gibson, R.L. and Layer, P.W., 1996. Further ^{40}Ar-^{39}Ar stepheating dating of fault rocks and metamorphic minerals from the Vredefort Dome and Witwatersrand Basin. In: *Abstracts XXVII. Lunar and Planetary Science Conference,* 1067-1068, Lunar and Planetary Institute, Houston.

Robb, L.J. and Meyer, F.M., 1991. A contribution to recent debate concerning epigenetic versus syngenetic mineralization processes in the Witwatersrand Basin. *Economic Geology.*, **86**, 396-401.

Robb, L.J. and Meyer, F.M., 1995. The Witwatersrand Basin, South Africa: geological framework and mineralisation processes. *Ore Geology Reviews,* **10**, 67-94.

Robinson, D., Bevins, R.E. and Rowbotham, G., 1993. The characterization of mafic phyllosilicates in low–grade metabasalts from eastern North Greenland. *American. Mineralogist*, **78**, 377-390.

Schreyer, W. and Bisschoff, A.A., 1982. Kyanite as a metamorphic mineral in the Witwatersrand sediments at Johannesburg and Krugersdorp, South Africa. *Transactions of the Geological Society of South Africa*, **85**, 211-214.

Stevens, G., Gibson, R.L. and Droop, G.T.R., 1997a. Mid–crustal granulite facies metamorphism in the Central Kaapvaal craton: the Bushveld Complex connection. *Precambrian Research*, **82**, 113– 132.

Stevens, G., Boer, R. and Gibson, R.L., 1997b. Metamorphism, fluid–flow, and gold mineralization in the Witwatersrand Basin: towards a unifying model. *South African Journal of Geology*, **100**, 363-375.

Tweedie, K.A.M., 1986. The Evander goldfield. *In:* Mineral Deposits of Southern Africa. C.R. Anhaeusser and S. Maske. (Eds). *Geological Society of South Africa*, 705–730.

Wallmach, T. and Meyer, F.M., 1990. A petrogenetic grid for metamorphosed aluminous Witwatersrand shales. *South African Journal of Geology,* **93**(1), 93–102.

Young, R.B., 1917. *A Study of the Auriferous Conglomerates of the Witwatersrand and Associated Rocks.* Gurney Jackson, London, 125pp.

Zang, W. and Fyfe, W.S., 1995. Chloritisation of the hydrothermally altered bedrock at the Igarape Bahia gold deposit, Carajas, Brazil. *Mineralium Deposita,* **30**, 30- 8.

Zhou, T. and Phillips, G.N., 1994. Sudoite in the Archaean Witwatersrand Basin. *Contributions to Mineralogy and Petrology,* **116**, 352-359.

Zhou, T., Dong, G. and Phillips, G.N., 1994. Chemographic analysis of assemblages involving
pyrophyllite, chloritoid, chlorite, kaolinite, kyanite, quartz: application to metapelites in the Witwatersrand goldfields, South Africa. *Journal of Metamorphic Geology,* **12**, 655–666.

_____oOo_____